Hydroxyl-Functionalized and N-Doped Multiwalled Carbon Nanotubes Decorated with Silver Nanoparticles Preserve Cellular Function

Alicia B. Castle,[†] Eduardo Gracia-Espino,[‡] César Nieto-Delgado,[‡] Humberto Terrones,[∥] Mauricio Terrones,[§,⊥,*] and Saber Hussain[†,*]

[†]AFRL/711HPW/RHPB, Wright-Patterson Air Force Base, Ohio 45433-5707, United States, [‡]Advanced Materials Department, IPICYT, Camino a la Presa San José 2055, San Luis Potosí 78216, México, [§]Research Center for Exotic Nano Carbons (JST), Shinshu University, 4-17-1 Wakasato, Nagano City 380-8553, Japan, [∥] Institute of Condensed Matter and Nanosciences (IMCN), Université Catholique de Louvain, Place Croix du Sud 1, B-1348 Louvain-la-Neuve, Belgium, and [⊥] Department of Physics, Department of Materials Science and Engineering & Materials Research Institute, The Pennsylvania State University, University Park, Pennsylvania 16802-6300, United States

ABSTRACT The present study aims to investigate biocompatibility of silver nanoparticles (Ag-NPs) anchored to different types of multiwalled carbon nanotubes (MWNTs). The MWNTs were decorated with Ag-NPs *via* a novel chemical route without using any sulfur containing reagent. Three different MWNTs were used as substrate materials for anchoring Ag-NPs: MWNTs-Ag (pure carbon), CO*x*-MWNTs-Ag (carboxyl functionalized), and CN*x*-MWNTs-Ag (nitrogen-doped). The Ag-NPs, synthesized without thiol capping groups, and which were strongly anchored to the nanotubes surfaces, exhibit an average size of 7 ± 1, 10 ± 1, and 12 ± 1 nm in MWNTs, CO*x*-MWNTs, and CN*x*-MWNTs, respectively. To determine biocompatibility of these three types of novel hybrid Ag-nanotube materials, cellular function and immune response were evaluated in the human keratinocyte cell line (HaCaT). Cellular assays revealed marginal toxicity after 24 h, and full cellular recovery was observed at 48 h based on an MTS assay for cellular viability. Therefore, Ag-nanotube systems appear to be very different from isolated dispersed Ag-NPs, and due to the strong interactions between the Ag-NPs and the doped nanotube surfaces, they make the Ag particles less toxic because they are not released easily to the cells. Pure carbon MWNTs appear to start releasing Ag-NPs at periods longer than 1 week by an observed decrease in cell proliferation. However, the use of N- and CO*x*-doped MWNTs do not appear to release Ag-NPs to the cells due to the strong binding to the tube surfaces caused by the doped sites. We envisage the use of CO*x*-MWNTs, and CN*x*-MWNTs anchored with Ag-NP as efficient drug delivery carriers and biosensors.

KEYWORDS: Ag nanoparticles · anchoring · nanotubes · biocompatibility · doping · HaCaT · toxicity · drug delivery

Biological functionalization of nanomaterials has attracted great attention in recent years because of the nanomaterials application in imaging and signaling pathway detection systems[1] and as a platform for the development of biosensors and drug deliverers. Multiwalled carbon nanotubes (MWNTs) have the unique ability to be functionalized[2] and well dispersed in aqueous media with various nanoparticles (*e.g.*, Ag) and chemical groups, and therefore be used as delivery vehicles. However, because of their toxicity there is a great need to develop modification options to increase their biocompatibility. If the nanomaterials are biocompatible, they can be used as specific capture agents, which can be of advantage in biological systems.

Ag nanoparticles (Ag-NPs) possess a high extinction coefficient, high surface plasmon resonance and antimicrobial properties and may be less toxic than the bulk form.[3,4] Currently, isolated and well-dispersed Ag-NPs have a variety of uses in everyday life such as Ag-NP infused storage containers,[5] Ag-NPs used to coat medical devices to reduce hospital related infections,[6] and applications in bandages,[7] footwear[8] and countless household items which claim to be antimicrobial. Owing to nanosilver's high surface plasmon resonance, it could be applied to many color-based biosensor applications and different lab-on-a-chip sensors. While all of these properties appear to make nano-Ag the new "miracle" of the nanotechnology world, other issues have been developing.

Ag-NPs have been shown to be toxic in a size-dependent manner according to Carlson *et al.*[9] The size dependent toxicity has been shown to be due to reactive oxygen species (ROS) production. A decrease in the membrane integrity allows the leakage of ROS outside the cell and leads to apoptosis.[9] Another mechanism of Ag-NP toxicity is believed to be due to the strong affinity of Ag to thiol groups.[10] The thiol groups are the functional groups of the amino acid

* Address correspondence to mtterones@shinshu-u.ac.jp, mut11@psu.edu, Saber.hussain@wpafb.af.mil.

Received for review May 13, 2010 and accepted March 2, 2011.

Published online March 02, 2011
10.1021/nn200178c

cysteine, and are considered highly reactive. In an effort to make the silver more biocompatible, Ag-NPs have been coated with polysaccharide,[11] but overtime the coating dissolves in the body again, thus rendering the cell to the toxic properties of the isolated uncoated Ag-NPs. Braydich-Stolle[12] showed that silver 10 nm-polysaccharide coated (Ag-10-PS) and silver 15 nm-hydrocarbon coated (Ag-15-HC) nanoparticles caused the same decrease in cell viability after a 6 day exposure in neuronal cells. If the coating is dissolving after 6 days in the media; it may be dissolving quicker in the human body.[12] An alternative method for making Ag-NPs more biocompatible could be by strongly anchoring them on MWNTs, so that the material could be easily dispersed and functionalized. In this context, Grabinski *et al*. showed that the toxicity of the carbon nanotubes is caused by the amount of iron left in the carbon nanotubes, rather than from the nanotubes themselves.[13]

In view of the extensive biomedical applications of Ag-NPs, including their potential as drug deliverers, this manuscript discusses the possibility of decorating MWNTs with Ag, in order to reduce the toxicity of Ag particles, thus preserving cellular function. Ag-NPs are used in several types of bandages and clothing, and therefore the Ag-NPs will readily come in contact with the skin. In our studies, human Keratinocytes (HaCaT) cells were chosen due to the likely contact of Ag-NPs with the skin.

RESULTS AND DISCUSSION

MWNTs have potential use as an imaging agent or as a biosensor because of the near-infrared emission to which they are able to respond.[14] The addition of different elements or functional groups to the nanotube network results in the modification of chemical, electronic, and mechanical properties within carbon nanotubes, thus increasing the chances for being used in future applications. Detection using MWNTs would allow greater tissue penetration and reduce fluorescent background. The present study examined the biocompatibility of three different hybrid systems: pure carbon MWNTs decorated with Ag nanoparticles (a known antimicrobial agent), nitrogen-doped MWNTs (CN*x*-MWNTs) coated with Ag, and MWNTs with oxygenated functional groups, such as carboxyl (CO*x*-MWNTs), anchoring Ag-NPs.

The CN*x*-MWNTs are more chemically reactive in the presence of oxygen at elevated temperatures when compared to pure carbon MWNTs, due to the incorporation of nitrogenated sites in their structure.[1,15,16] The presence of carbonyl, hydroxyl, and oxygenated functional groups on the CO*x*-MWNTs surface also enhances their reactivity toward oxygen and other species, in addition to enhanced solubility.[17] In this context, we have carried out thermogravimetric (TGA) analysis, in which CN*x*-MWNTs exhibited faster oxidation than MWNTs and CO*x*-MWNTs. These results

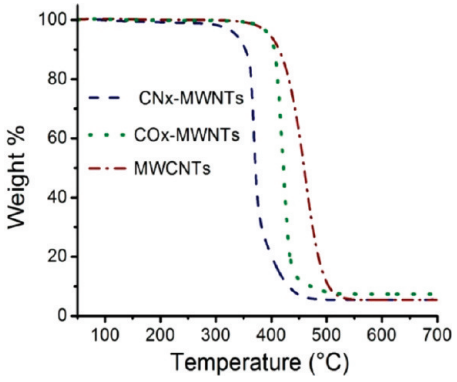

Figure 1. TGA analysis of undoped and doped MWNTs in O_2. It can be observed that CN*x*-MWNTs decomposed first exhibiting a faster oxidation rate than CO*x*-MWNTs and MWNTs. The materials reveal a decomposition temperature of of 370 °C for CN*x*-MWNT and 420 and 460 °C for CO*x*-MWNTs and MWNTs, respectively.

TABLE 1. EDX Analysis and Others Characteristics of Carbon Nanotubes

	CN*x*-MWNTs	CO*x*-MWNTs	MWNTs
length[a] (μm)	81 ± 24	451 ± 74	588 ± 41
diameter[a] (nm)	30 ± 9	33 ± 15	46 ± 21
$T_{decomposition}$[b](°C)	370	420	460
atom % C	96.5	95.75	97.33
atom % N	1.90	0	0
atom % O	1.29	3.77	1.74
atom % Fe	0.31	0.48	0.93

[a] Length and diameter were obtained from SEM images. [b] Data obtained by TGA analysis in air.

suggest that CN*x*-MWNTs and CO*x*-MWNTs exhibit more reactive sites when compared to pure (undoped) MWNTs (Figure 1.). These sites could interact in different ways with their surrounding environment, thus modifying significantly their interaction with certain types of molecules. Energy dispersive X-ray (EDX) analyses were also performed in order to confirm the functionalization of the materials. These results and other physical characteristics of MWNTs are shown in Table 1. The reactivity observed could be summarized as follows: MWNTs < CO*x*-MWNTs < CN*x*-MWNTs. Figure 2 shows TEM micrographs of the nanotubes-Ag composites: Panels a and b depict the MWNTs-Ag material, and it can be observed a homogeneous distribution of Ag particles on the tubes surface; Figure 2 panels c and d show CO*x*-MWNTs-Ag and panels e and f show CN*x*-MWNTs-Ag at high magnifications. It can be observed that all Ag-NPs are well anchored to the surfaces of the nanotubes and do not exhibit any coating material at very high magnifications. Figure 3 depicts the size distribution of the Ag-NPs attached in the three different nanotubes; the average particle size obtained by a logNormal fit was 7 ± 1 nm for MWNTs-Ag, 10 ± 1 nm for CO*x*-MWNTs-Ag, and 12 ± 1 nm in CN*x*-MWNTs-Ag. We also carried out X-ray powder diffraction

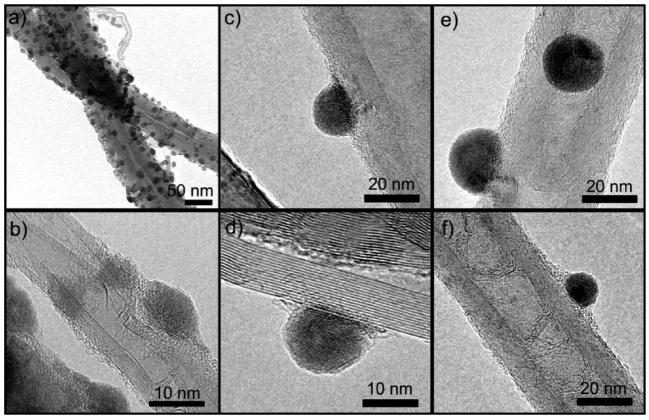

Figure 2. TEM micrographs of MWNTs-Ag (a,b); CO*x*-MWNTs-Ag (c,d), and CN*x*-MWNT-Ag (e,f). (a,b) high load of Ag-NPs anchored onto the nanotubes walls; (c-d) CO*x*-MWNTs-Ag composite; the good interaction of the Ag-NP with the nanotube is evident. (e-f) CN*x*-MWNTs shows the bamboo-like structure generated by the introduction of nitrogen. In all cases, the Ag-NPs exhibit the absence of a coating layer.

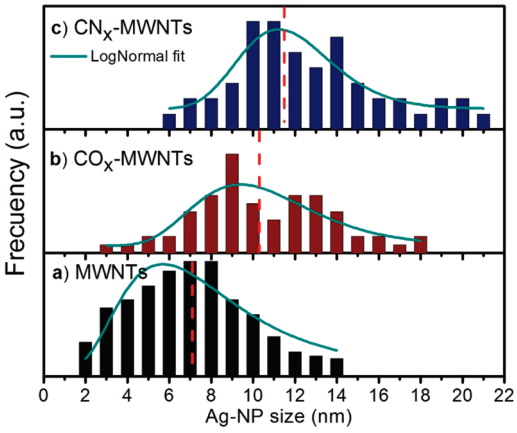

Figure 3. Ag-NPs size distribution of (a) MWNTs, (b) CO*x*-MWNTs, and (c) CN*x*-MWNTs composites. The dashed lines represent the average particle size obtained by fitting the data with a logNormal distribution (solid line). The mean size for MWNTs is 7 ± 1; CO*x*-MWNTs, 10 ± 1; and CN*x*-MWNTs, 12 ± 1 nm.

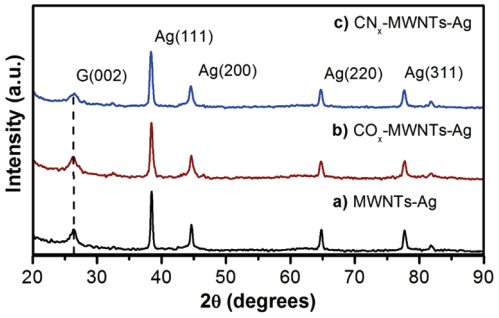

Figure 4. X-ray powder diffraction patterns of the three different hybrid nanomaterials. (a) MWNTs-Ag, (b) CO*x*-MWNTs-Ag, and (c) CN*x*-MWNTs-Ag. The peak located at ~26° corresponds to the (002) planes of graphite, the other peaks belong to Ag nanocrystals, which exhibit the face centered cubic structure.

(XRD) analyses of the three Ag-nanotube systems. Here, the corresponding peaks of the Ag-NPs exhibit the face-centered-cubic structure corresponding to Ag (see Figure 4). The XRD and the HRTEM analyses clearly demonstrate the presence and the anchoring of Ag-NPs on the surface of the tubes and the absence of coating within the Ag-NPs.

Changes in the inflammatory response can provide an insight into the state of the cellular environment and be an indicator of cellular stress. HaCaT cells were chosen because many Ag products come in contact with the skin, and therefore human keratinocytes seem the most realistic for this type of exposure. HaCaT cells typically produce IL-6 and TNF-α in response to stress so these cytokines were chosen to be measured.[13] IL-6 and TNF-α primers were ordered from Integrated DNA Technology (IDT). Figure 5 shows the polymerase chain reaction (PCR) results at 6 h of the hybrid nanomaterials exposure and illustrates slight increases in TNF-α and IL-6 when compared to the control. The MWNT-Ag, CN*x*-MWNT-Ag, and CO*x*-MWNT-Ag all showed a small initial increase in IL-6 and TNF-α, but it was not significant. After 24 h, the increase in IL-6 did not change in any of the treatment groups, but TNF-α continued to increase (Figure 5) in the MWNT-Ag and CO*x*-MWNTs-Ag. This may be due to IL-6 stimulating the immune response of TNF-α, thus leading to inflammation and cell death. Because of the recovery assays we performed, it was evident the cells had the ability to recover.[18,19] Further time points were not evaluated since we also had available the MTS results. If the cells were still having a strong immune response at 48 h, the cells would be significantly decreasing in viability, and we would therefore observe a great reduction in cell proliferation. In addition, the lack of change in CytoViva Images (see Figure 6) provided evidence that the cellular structure was very similar to the control samples. Mitochondrial membrane potential (MMP) was examined to determine the initial toxicity due to ROS production. ROS production could not be measured accurately due to interactions observed between the functionalized MWNTs and the reagents. Multiple kits were used, but ROS was shown

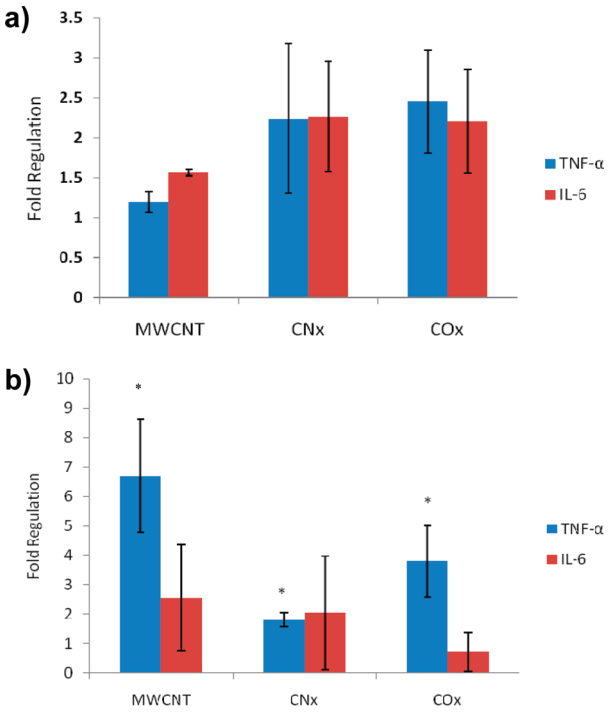

Figure 5. Change in inflammatory cytokine expression following (a) 6 and (b) 24 h exposure to nanomaterials. PCR results of inflammatory markers TNF-α and IL-6 in comparison to the β-actin housekeeping marker in HaCaT cells showed no significant increases at 6 h for TNF-α or IL-6 and a significant increase in TNF-α for MWNT-Ag and CO*x*-MWNT-Ag at 24 h of exposure. A *p*-value < 0.05 was considered statistically significant (∗) using the Student's *t*-test.

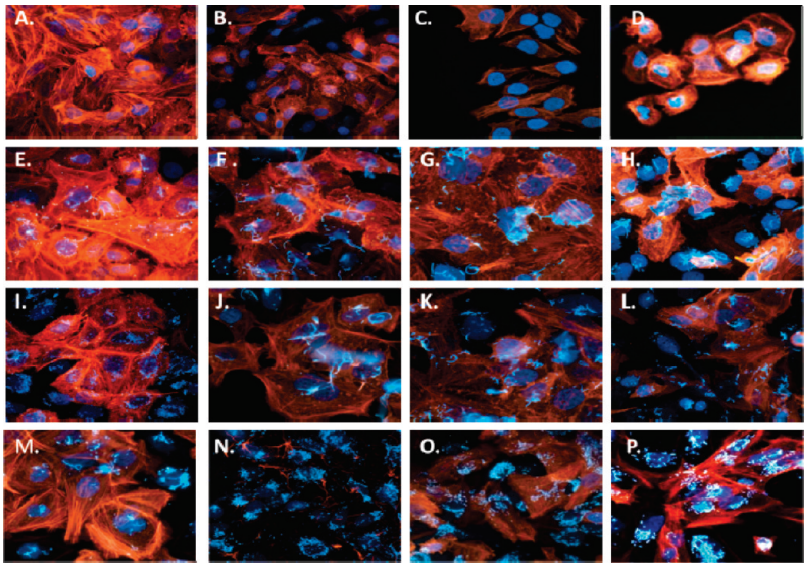

Figure 6. CytoViva imaging of HaCaT cells dosed with 25 μg/mL nanomaterials and then stained for actin Control HaCaT cells at (A) 24 h, (B) 48 h, (C) 72 h and (D) 1 week. MWNTs-Ag at (E) 24 h, (F) 48 h, (G) 72 h and (H) 1 week. CN*x*-MWNTs-Ag at (I) 24 h, (J) 48 h, (K) 72 h, and (L) 1 week, and CO*x*-MWNTs-Ag at (M) 24 h, (N) 48 h, (O) 72 h, and (P) 1 week. Each picture with the MWNT composites shows localized nuclear binding with the nucleus stained blue and the actin filaments stained red/orange. The particles appear as the bright spots. There appears to be limited actin filament disruption in comparison to the control pictures. Binding can be determined based on the number of particles seen even after 1 week postexposure time in the exposure media.

to be produced a-cellularly. Mitochondrial membrane potential is a major component of the mitochondrial electrochemical proton gradient, and its maintenance/homeostasis is a good assessment of cellular function. The change in the MMP is a measure of uncoupling of the electron transport chain and a sign of cellular stress. When measuring the MMP after a 24 h period of the NT-AgNP systems exposure, a significant decrease in mitochondrial membrane potential was observed (Figure 7a). The significant decrease in MMP

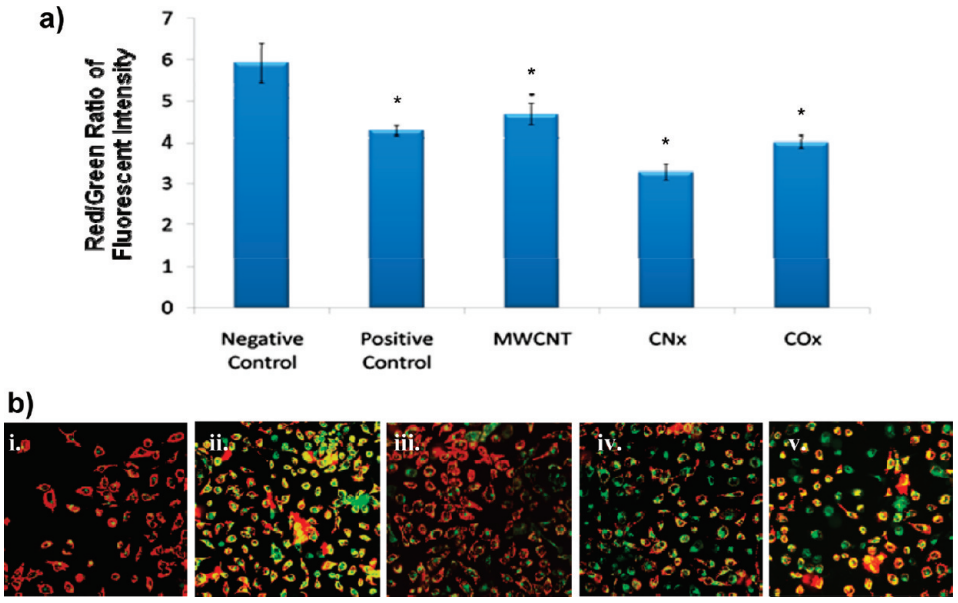

Figure 7. Reduction in mitochondrial membrane potential (MMP) after 24 h of exposure to 25 μg/mL of Ag-MWNT composites: (a) fluorescent intensity measurements of cells treated with Ag-MWNTs *verses* untreated HaCaT cells. The decreases in the ratio correspond to a decrease in MMP. An asterisk (*) shows a significant decrease; (b) qualitative confocal images of HaCaT cells (i) control, (ii) positive control, (iii) MWNT-Ag, (iv) CN*x*-MWNTs-Ag, (v) CO*x*-MWNTs-Ag; (*) *p*-values < 0.05 were considered statistically significant using the Student *t* test.

indicated a decrease in cell viability most likely due to oxidative stress. The decreases in MMP provide information that the cell is undergoing oxidative stress and possibly preparing to undergo apoptosis. Confocal microscope images revealed the same qualitative results as those seen in Figure 7a. The images showed more red fluorescence indicating a decrease in MMP for CN*x*-MWNT-Ag and CO*x*-MWNT-Ag than the control (Figure 7b), and also slightly more red fluorescence in the MWNT-Ag sample, thus representing a reduction in mitochondrial membrane potential (Figure 7b). Control cells showed no red fluorescence, while the positive controls showed high amounts of red fluorescence demonstrating that the test was performed adequately (Figure 7b). The positive control for the experiment was hydrogen peroxide. The CN*x*-MWNT-Ag showed the greatest reduction in MMP but the least increase in immune response.

Figure 8 shows the MTS (3-(4,5-dimethylthiazol-2-yl)-5-(3-carboxymethoxyphenyl)-2-(4-sulfophenyl)-2*H*-tetrazolium) results of the HaCaT cells exposed to varying concentrations of AgNPs−nanotube systems for 24 h, and their subsequent recovery. The cells have completely recovered from the exposure after 48 h (Figure 8). The decreases in cellular viability observed after 72 h and 1 week are likely caused by the cells having a large increase in viability at 48 h and becoming over confluent, thus causing cell death. Cell viability could also have decreased because Ag-NPs could have detached after 1 week from the tubes, especially those that had not been doped or functionalized (pure MWNTs).

While the cells show this initial inflammatory response due to the presence of the foreign hybrid Ag-nanotube systems, we observed that they also have an ability to recover over time. The inflammatory response appears to help the cells to recover from the exposure, rather than sending the cells directly into apoptosis. Therefore, the detachment of AgNPs is not occurring with our hybrid nanotube−AgNP systems, especially the CO*x*-MWNTs-Ag. After the 48 h time point, we do observe a decrease in cellular viability, especially for MWNTs-Ag, and this could be explained in terms of the release of some Ag-NPs that were not strongly anchored to the pure MWNTs due to the lack of dopants (or reactive sites) on the tube surfaces.

Figure 6 shows all three types of MWNTs decorated with Ag-NPs interacting with cells and appearing to bind to the nucleus or nuclear region, based on the CytoViva imaging. We determined the interaction was due to the high concentration of MWNTs in the images taken after 1 week. The cells were washed and placed in exposure media for a week, and thus if binding was not occurring there would be no MWNTs. The human keratinocytes appeared to exhibit actin filament disruption caused by the MWNTs-Ag. However, the MTS results showed no toxicity, but rather an increase in cell viability. The actin filament disruption is likely due to the exposure media, because the cells do not grow normally due to the lack of fetal bovine serum (FBS). This is also indicated in the control cells, which appear to become rounded over time. The ability of human keratinocytes to recover after an acute exposure demonstrates that these Ag−nanotube systems behave differently from isolated AgNPs and isolated MWNTs, and therefore have the possibility for being used as drug deliverers even after experiencing an initial mild

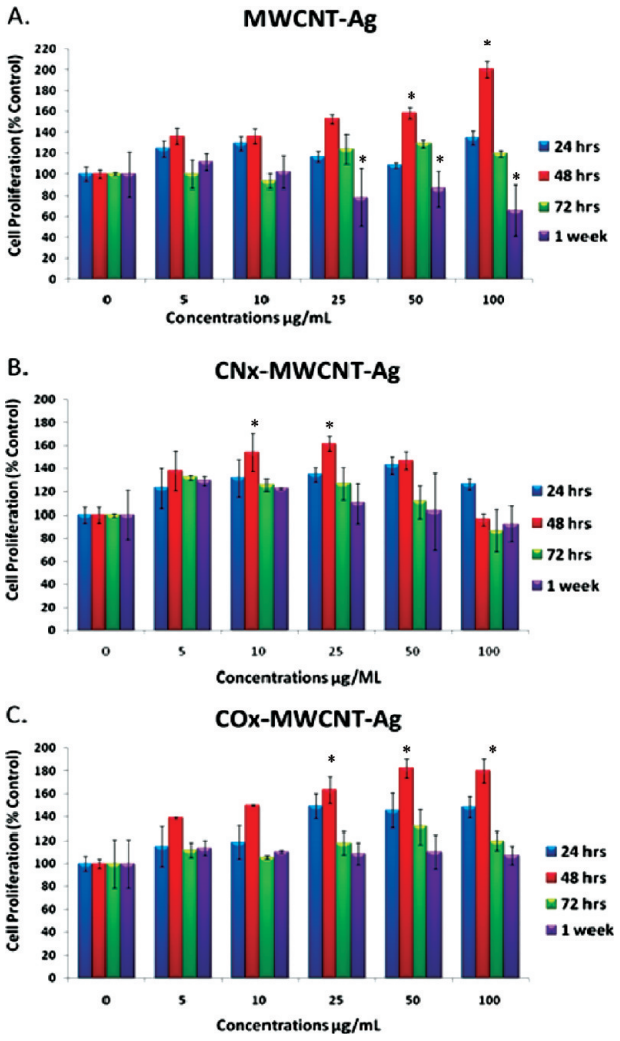

Figure 8. Cell viability in HaCaT cells exposed to different MWNT composites. The cells were exposed to concentrations of 0, 5, 10, 25, 50, and 100 μg/mL solutions of (A) MWNT-Ag, (B) CN*x*-MWNTs-Ag, and (C) CO*x*-MWNTs-Ag for 24 h and washed . Recovery was then examined at 24 h, 48 h, 72 h, and 1 week; (*) *p*-values < 0.05 were considered statistically significant using the Student's *t*-test.

TABLE 2. Summary Table Showing Particle Size, Cellular Morphology, Change in Mitochondrial Membrane Potential (MMP), Inflammatory Response, and Recovery[a]

				PCR 6 h fold increase		PCR 24 h fold increase		
particle type	ave diameter (nm)	cell morphology	MMP	IL-6	TNF-α	IL-6	TNF-α	MTS recovery cell proliferation
Ag-MWNT	6.64	minor action disruption, nuclear binding	* decrease	1.5	1.3	2.7	6.8	increase
Ag-CN*x*-MWNT	8.82 and 12.70	no disruption, nuclear binding	* decrease	2.4	2.4	2	1.9	increase
Ag-CO*x*-MWNT	10.70 and 13.94	no disruption, nuclear binding	* decrease	2.6	2.5	0.5	4	increase

[a] There was a significant (*) decrease in MMP as well as a significant increase in TNF-α at 24 h for Ag-MWNT and Ag-MWNT-CO*x*.

toxicity. Table 2 shows the summary of the acute exposure to the novel hybrid nanomaterials.tpb

Isolated Ag-NPs have been shown to be toxic in a size-dependent manner. In particular Ag-15 has been demonstrated to be toxic to BRL-3A cells, C18-4 cell, and macrophages. Ag-15 has been shown to be toxic regardless of the coating, which was in agreement with the results that Ag toxicity increases with size reduction.[11,12] Silver is the most toxic at small sizes due to its ability to produce more ROS at these sizes. The Ag-NPs used in this study were under 30 nm and should have been toxic in a dose-dependent manner. All reports in the literature have shown an unavoidable toxicity if they are isolated. When comparing ROS production and cell viability between previous studies and our study at the same concentrations and time

points, we observed a much greater increase in biocompatibility in the novel Ag−nanotube systems rather than isolated Ag-NPs. In addition, the synthesis of small Ag-NPs without using thiol groups was not possible in the absence of MWNTs; only agglomerates of large (micrometer size) Ag-NPs resulted, and these materials could not be compared with the MWNTs-Ag systems studied here. Therefore, the presence of MWNTs are crucial for obtaining a uniform anchorage (surface dispersion) of Ag-NPs of small sizes (*e.g.*, < 10 nm), which could then be used for drug delivery applications.

All three carbon nanotubes were coated with Ag-NP, but interestingly those Ag systems containing the pure MWNTs did not increase biocompatibility at higher doses, possibly due to the release of some Ag-NPs at longer times. MWNTs with nitrogen and carbonyl groups resulted in an efficient (strong) anchorage of the AgNPs, and a resulting stability of hybrid Ag−nanotube materials with human cells. The released Ag-NPs from pure MWNT tubes after long periods are also expected to interact with proteins or cell structures that may lead to the inhibition of cellular processes, causing the slight reduction in cell viability.

In a study performed by Cheng *et al*,[20] the acute and long-term effects of functionalized MWNTs were examined in zebrafish. In the early stages, the zebrafish generated an immune response due to accumulating white blood cells. The zebrafish that were exposed to the MWNTs produced an initial response, but the nanotubes were cleared from their body after 96 h. These results agree with ours showing a significant inflammatory response followed by the cells capacity for recovery. However, the second generation of the zebrafish had a lower survival rate suggesting that MWNTs had no significant toxicity initially but could display long-term effects on the progeny, and further clarification is still required in this context when exposing these novel Ag−nanotube systems.

It is important to mention that tests with the three nanotube types without Ag-NP were also carried out, and we found that at concentrations as high as 10 μg/mL, the cellular functions were not inhibited (results not shown here). Therefore, the presence of Ag-NPs, tightly anchored to the nanotube surfaces and without the presence of thiol groups, only reveals some inflammatory signs followed by the cell's full recovery.

In summary, the three novel Ag−nanotube systems studied here did not show a significant change in cellular functions (especially at doses lower than 10 μg/mL), thus confirming that they could be used in the future as drug delivery agents. Only pure carbon MWNTs-Ag systems start to release Ag nanopartciles at periods longer than one week by an observed decrease in cell proliferation. It is noteworthy that these Ag-nanotube systems are very different from isolated and dispersed Ag-NPs capped with thiol groups, and appears that the strong interactions between the Ag-NPs (without thiol groups) and the nanotube surfaces make the Ag particles less toxic (not able to be released to the cells). Therefore, nanoscale materials hold the key to several unopened doors in the science field, but several questions still need to be answered. Is the possibility of a toxic reaction worth the risk? Further biocompatibility assays need to be performed before Ag-nanotube systems can be considered for medical or biological uses. If functionalized carbon nanotubes are biocompatible the possibilities are endless.

EXPERIMENTAL SECTION

The multiwalled carbon nanotubes (MWNTs) used in this study have been doped with nitrogen or carbonyl groups and then decorated with Ag nanoparticles.

The nanotubes were synthesized using a chemical vapor deposition (CVD) method: The pure MWNTs were synthesized by the thermal decomposition of a mixture of 2.5 wt % of ferrocene ($FeCp_2$; 98% Aldrich) and toluene (C_7H_8; 99.9% Fermont) at 825 °C in an Ar atmosphere for 30 min, following the method described elsewhere.[21,22] Similarly, nitrogen-doped multiwalled carbon nanotubes (CN*x*-MWNTs) were obtained by decomposition of a solution containing 2.5 wt % of ferrocene and benzylamine (C_7H_9N; 99% Sigma-Aldrich).[14] Finally, ethanol-based (carbonyl and carboxyl-functionalized) carbon nanotubes (CO*x*-MWNTs) were produced using a solution of ferrocene (2.5 wt %), 1 wt % of ethanol (CTR scientific), and toluene (C_7H_8).[16]

The three different types of nanotubes tested in this work were used without any chemical modification (*e.g.*, water or acid treatments). The anchorage procedure consisted of adding 1 mg of the nanotubes to a solution of acetone (C_3H_6O; 20 mL) and silver nitrate ($AgNO_3$; 83 μL from a solution 0.1 N, J.T. Baker) in a flask. Subsequently, the suspension was dispersed ultrasonically for 1 h. The solution was then placed in a water bath to increase the temperature to ~54 °C, and at this point 10 mL of *N*, *N*-dimethylformamide (DMF, 99% Sigma-Aldrich) were added as a reducing agent; the temperature of the uniform suspension was maintained for 20 additional minutes. Subsequently, the nanotube samples were centrifuged, washed with distilled water twice, and dried at 70 °C in an oven.

The characterization of the Ag−nanotube uniform dispersions were carried out by scanning electron microscopy (FEG-SEM, FEI XL30 FEG/SFEG) operated at 15 kV. The thermogravimetric analyses (TGA, Thermo-Haake, Cahn VersaTherm Hs) were carried out heating at 10 °C/min to 800 °C in air. The X-ray powder diffraction pattern of all samples were performed using a XRD D8 ADVANCE−BRUKER AXS, with a Cu K_α radiation (λ = 1.54060 Å). The operating current and voltage were maintained at 35 kV and 25 mA. High resolution images were taken with a HRTEM-field emission Tecnai F30 operating at 300 keV.

To estimate the amount of Ag-NPs on the surface of the different tubes, we have used the average diameters of the different Ag-NPs (7 nm for MWNTs-Ag, 10 nm for CO*x*-MWNTs-Ag, and 12 nm for CN*x*-MWNTs-Ag), and considered that the

particles are spheres, and then calculated the volume for each sphere. Subsequently, we used the bulk density of Ag, and by considering that in 100 mg of MWNTs, *ca.* 1 mg of Ag is contained (estimated by EDX analysis), we calculated the total amount of nanotubes for each sample: (a) for MWNTs-Ag, $\sim 5.3 \times 10^{14}$ Ag-NPs per 100 mg of MWNTs; (b) for CO*x*-MWNTs-Ag, $\sim 1.8 \times 10^{14}$ Ag-NPs per 100 mg of nanotubes, and (c) for CN*x*-MWNTs-Ag, $\sim 1.0 \times 10^{14}$ Ag-NPs per 100 mg of nanotubes. If we then use doses of 25 μg/mL as a reference, we obtain the following: for MWNTs-Ag, $\sim 13.3 \times 10^{10}$ Ag-NPs per dose; for CO*x*-MWNTs-Ag, $\sim 4.5 \times 10^{10}$ Ag-NPs per dose, and for CN*x*-MWNTs-Ag, $\sim 2.6 \times 10^{10}$ Ag-NPs per dose.

HaCaT cells were donated generously by Dr. James F. Dillman III, of the U.S. Army Medical Research Institute of Chemical Defense. The HaCaT cells were maintained in RPMI-1640 with 1% penicillin-streptomycin and 10% FBS at 37.0 °C and 5% CO_2.[23] The cells were passaged using Trypsin-EDTA and PBS when they reached 70−80% confluency. For nanomaterial exposures, RPMI media supplemented with 1% penicillin/streptomycin was used. The inflammatory response of the HaCaT cells to the nanotubes was measured using real-time PCR. IL-6 and TNF-α primers were ordered from Integrated DNA Technology (IDT) and used for PCR.

Cells were plated at 300 000 cells/mL in six-well plates and dosed with 25 μg/mL of the different nanomaterials dispersed in water, for 6 h and 24 h. After each time point the RNA was isolated using the Qiagen RNA isolation kit. The isolated RNA was then NanoDropped to determine the amount of RNA present in the sample. Then 1 μg of RNA was used in real time PCR analysis. The Express Script from Invitrogen was used, and 100 nM forward and reverse primers for TNF-α, IL-6, and beta actin were used. On the Stratagen MX3005P the RNA was reverse transcribed for 30 min at 50 °C and then amplified using a cycle of 94 °C for 30 s, 60 °C for 1 min at 40 cycles. The TNF-α, IL-6 expression was normalized based on beta actin expression. The 6 h and 12 h time points were chosen, because if the cells are still producing a strong immune response after these time points we will see decreases in cell viability, which would be evident in MTS assays.

The mitochondrial membrane potential was measured to examine changes in the mitochondrial membrane, which correlates to ROS production and apoptosis. The cells were exposed to 25 μg/mL of Ag−nanotubes, dispersed in water, for 24 h. The protocol from the Mit-E-Ψ Mitochondrial Permeability Detection Kit (AK-116) was used throughout the assay. The cells were imaged using the confocal microscope and MMP was measured on the basis of images and computer software, which compares the fluorescent intensity of each well to the control.

CytoViva imaging was used to determine the interaction between the Ag−nanotube systems and the cells as previously described.[24]

Cell viability was assayed by MTS as indicated by the CellTiter 96AQueous One Solution from Promega, which measures mitochondrial function and directly correlates to cell viability. The relative cell viability (%) related to control wells containing cell culture exposure media without nanoparticles was calculated by [A]test/[A]control × 100, where [A]test is the absorbance of the test sample and [A]control is the absorbance of control sample. Each experiment was done in triplicate.

Statistical analysis was performed on each of the cellular assays. The tests were run three times each and each sample was performed in triplicate. A Student *t* test was performed with all of the samples and *p*-values < 0.05 were considered significant.

Acknowledgment. This work was supported by the Air Force Office of Scientific Research (AFOSR) Project (JON No. 2312A211). M.T. thanks JST-Japan for funding the Research Center for Exotic NanoCarbons, under the Japanese regional Innovation Strategy Program by the Excellence. This work was also sponsored by the U.S. Air Force grant FA9550-08-1-0205, entitled "Biocompatibility and Toxicological Effects of Doped, Functionalized, and Pure Carbon Nanotubes". CONACYT-Mexico support is also acknowledged for Ph.D. fellowships (E.G.E., C.N.D.). Ms. Castle was funded by the Consortium Research Fellows Program throughout this project.

Note Added after ASAP Publication. After this paper was published online March 16, 2011, a correction was made to the affiliation for author Humberto Terrones. The revised version was published April 1, 2011.

REFERENCES AND NOTES

1. Hernández-Sánchez, B. A.; Boyle, T. J.; Lambert, T. N.; Daniel-Taylor, S. D. Synthesizing Biofunctionalized Nanoparticles To Image Cell Signaling Pathways. *IEEE Trans. Nanobiosci.* **2006,** *5*, 222–230.
2. Challa, S. S. R. Kumar. Nanotechnologies for the life sciences. *Biofunctionalization of Nanomaterials*; Wiley VCH: Weinheim, Germany, 2005; pp 49−51.
3. Oberdörster, G.; Maynard, A.; Donaldson, K.; Castranova, V.; Fitzpatrick, J.; Ausman, K.; Carter, J.; Karn, B.; Kreyling, W.; Lai, D. Principles for Characterizing the Potential Human Health Effects from Exposure to Nanomaterials; Elements of a Screening Strategy. *Part. Fibre Toxicol.* **2005,** *2*, 8.
4. Thomas, K.; Sayre, P. Research Strategies for Safety Evaluation of Nanomaterials, Part I: Evaluating the Human Health Implications of Exposure to Nanoscale Materials. *Toxicol. Sci.* **2005,** *2*, 316–321.
5. www.sharperimage.com.
6. Alt, V.; Bechert, T.; Steinrucke, P.; Wagener, M.; Seidel, P.; Dingeldein, E.; Domann, E.; Schnettler, R. An *in Vitro* Assessment of the Antibacterial Properties and Cytotoxicity of Nanoparticulate Silver Bone Cement. *Biomaterials* **2004,** *25*, 4383–4391.
7. Georgia Institute of Technology, Copyright 2006 NNIN-1025, http://www.nnin.org/doc/NNIN-1025.pdf
8. Benn, T. M.; Weterhoff, P. Nanoparticle Silver Released into Water from Commercially Available Sock Fabrics. *Environ. Sci. Technol.* **2008,** *42*, 4133–4139.
9. Carlson, C.; Hussain, S. M.; Schrand, A. M.; Braydich-Stolle, L. K.; Hess, K. L.; Jones, R. L.; Schlager, J. J. Unique Cellular Interaction of Silver Nanoparticles: Size Dependent Generation of Reactive Oxygen Species. *J. Phys. Chem. B* **2008,** *112*, 13608–13619.
10. Hussain, S.; Meneghini, E.; Moosmayer, M.; Lacotte, D.; Anner, B. M. Potent and Reversible Interaction of Silver with Pure Na, K-ATPase and Na, K-ATPase-Liposomes. *Biochim. Biophys. Acta* **1994,** *2*, 402–408.
11. Schrand, A. M.; Braydich-Stolle, L. K.; Schlager, J. J.; Dai, L.; Hussain, S. M. Can Silver Nanoparticles Be Useful as Potential Biological Labels? *Nanotechnology*, 2008, *19*, 235104.
12. Braydich-Stolle, L. K.; Hussain, S. M.; Schlager, J. J.; Hofmann, M. C. *In Vitro* Cytotoxicity of Nanoparticles in Mammalian Germline Stem Cells. *Toxicol. Sci.* **2005,** *88*, 412–419.
13. Grabinski, C.; Hussain, S.; Lafti, K.; Braydich-Stolle, L.; Schlager, J. Effect of Particle Dimension on Biocompatibility of Carbon Nanotubes. *Carbon* **2007,** *45*, 2828–2835.
14. Barone, P. W.; Baiki, S.; Heller, D. A.; Strano, M. S. Near-Infrared Optical Sensors Based on Single-Walled Carbon Nanotubes. *Nat. Mater.* **2005,** *4*, 86–92.
15. Terrones, M.; Ajayan, P. M.; Banhart, F.; Blase, X.; Carroll, D. L.; Charlier, J. C.; Czerw, R.; Foley, B.; Grobert, N.; Kamalakaran, R.; *et al*.N-doping and Coalescence of Carbon Nanotubes: Synthesis and Electronic Properties. *Appl. Phys. A: Mater. Sci. Process.* **2002,** *74*, 355–361.
16. Lepró, X.; Vega-Cantú, Y. I.; Rodríguez-Macías, F. J.; Bando, Y.; Golberg, D.; Terrones, M. Production and Characterization of Coaxial Nanotube Junctions and Networks of CN*x*/CNT. *Nano Lett.* **2007,** *7*, 2220–2226.
17. Botello-Méndez, A. R.; Campos-Delgado, J.; Morelos-Gómez, A.; Romo-Herrera, J. M.; Rodríguez, A. G.; Navarro, H.; Vidal, M. A.; Terrones, H.; Terrones, M. Controlling the Dimensions, Reactivity and Crystallinity of Multiwalled Carbon Nanotubes Using Low Ethanol Concentrations. *Chem. Phys. Lett.* **2008,** *453*, 55–61.
18. Yoshizumi, M.; Nakamura, T.; Kato, M.; Ishioka, T.; Kozawa, K.; Wakamatsu, K.; Kimura, H. Release of Cytokines/Chemokines and Cell Death in UVB-Irradiated Human Keratinocytes, HaCaT. *Cell Biol. Int.* **2008,** *32*, 1405–1411.

19. Johnson, A.; Alberts, B.; Lewis, J.; Raff, M.; Roberts, K.; Walter, P. *Molecular Biology of the Cell*, Taylor and Francis: New York, NY; 2002.
20. Cheng, J. P.; Chan, C. M.; Veca, L. M.; Poon, W. L.; Chan, P. K.; Qu, L.; Sun, Y. P.; Cheng, S. H. Acute and Long-Term Effects after Single Loading of Functionalized Multiwalled Carbon Nanotubes into Zebrafish (*Danio rerio*). *Toxicol. Appl. Pharmacol.* **2009,** *235*, 216–225.
21. Pinault, M.; Mayne-L'Hermite, M.; Reynaud, C.; Beyssac, O.; Rouzaud, J. N.; Clinard, C. Carbon Nanotubes Produced by Aerosol Pyrolysis: Growth Mechanisms and Post-Annealing Effects. *Diam. Relat. Mater.* **2004,** *13*, 1266–1269.
22. Mayne, M.; Grobert, N.; Terrones, M.; Kamalakaran, R.; Rühle, M.; Kroto, H. W.; Walton, D. R. M. Pyrolytic Production of Aligned Carbon Nanotubes from Homogenously Dispersed Benzene-Based Aerosols. *Chem. Phys. Lett.* **2001,** *338*, 101–107.
23. Boukamp, P.; Petrussevska, R. T.; Breitkreutz, D.; Hornung, J.; Markham, A.; Fusenig, N. E. Normal Keratinization in a Spontaneously Immortalized Aneuploid Human Keratinocyte Cell Line. *J. Cell Biol.* **1988,** *106*, 761–771.
24. Skebo, J. E.; Grabinski, C. M.; Schrand, A. M.; Schlager, J. J.; Hussain, S. M. Assessment of Metal Nanoparticle Agglomeration, Uptake, and Interaction Using High-Illuminating System. *Int. J. Toxicol.* **2007,** *26*, 135–141.